2009-24-0067

Rule-Based Optimization of Intermittent ICE Scheduling on a Hybrid Solar Vehicle

Gianfranco Rizzo, Marco Sorrentino, Ivan Arsie
Department of Mechanical Engineering, University of Salerno, 84084 Fisciano (SA), Italy

ABSTRACT

In the paper, a rule-based (RB) control strategy is proposed to optimize on-board energy management on a Hybrid Solar Vehicle (HSV) with series structure. Previous studies have shown the promising benefits of such vehicles in urban driving in terms of fuel economy and carbon dioxide reduction, and that economic feasibility could be achieved in a near future.

The control architecture consists of two main loops: one external, which determines final battery state of charge (SOC) as function of expected solar contribution during next parking phase, and the second internal, whose aim is to define optimal ICE-EG power trajectory and SOC oscillation around the final value, as addressed by the first loop.

In order to maximize the fuel savings achievable by a series architecture, an intermittent ICE scheduling is adopted for HSV. Therefore, the second loop yields the average power at which the ICE is operated as function of the average values of traction power demand and solar power. Expected solar contribution can be estimated starting from widely available solar databases and by processing past solar energy data measured on the vehicle. Neural Networks predictors, previously stored data and/or GPS derived information are suitable to estimate average power requested for vehicle traction.

Extensive simulation analyses were carried out to test the performance of the RB algorithm, also comparing it to Genetic Algorithms-based optimization strategies previously developed by the authors. The results confirm the high potentialities offered by the proposed RB control strategy to perform real-time energy management on hybrid solar vehicles.

The proposed rule-based optimization is currently under-implementation in an NI® cRIO control unit, thus allowing to perform experimental tests on a real HSV prototype developed at University of Salerno.

INTRODUCTION

In the last years, there is an increasing awareness about the need to achieve a more sustainable mobility, allowing meeting the mobility needs of the present without compromising the ability of future generations to meet their needs [1]. The most pressing arguments towards new solutions for personal mobility are the following:

- fossil fuels, largely used for car propulsion, are doomed to depletion, and their price is subject to large and unpredictable fluctuations (see Figure 1);

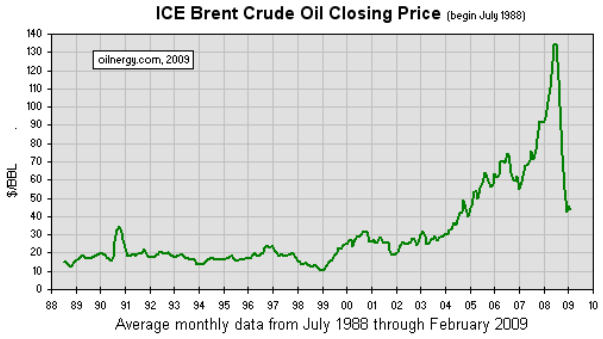

Figure 1 - *Trends in oil price (http://www.oilnergy.com/1obrent.htm).*

- the CO_2 generated by the combustion processes occurring in conventional thermal engines contributes to the greenhouse effects, with dangerous and maybe dramatic effects on global warming and climatic changes;
- the worldwide demand for personal mobility is rapidly growing, especially in China (see Figure 2) and India; as a consequence, energy consumption and CO_2 emissions related to cars and transportation are increasing;

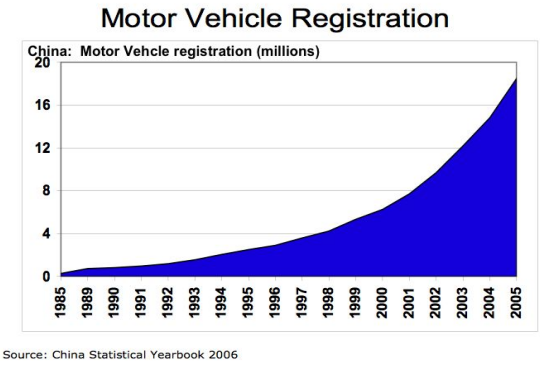

Figure 2 - *Motor vehicle registration in China (Millions).*

One of the most realistic short term solutions to the reduction of gaseous pollution in urban drive, as well

as the energy saving requirements, is represented by Hybrid Electric Vehicles (HEV). These vehicles, that have evolved to industrial maturity, allow achieving significant benefits in terms of fuel economy, but still using fossil fuels. On the other hand, in recent years increasing attention is being spent towards the applications of solar energy to electric and also to hybrid cars. But, while pure solar vehicles do not represent a practical alternative to cars for normal use, the concept of a hybrid electric car assisted by solar panels appears more realistic. The reasons for studying and developing a Hybrid Solar Vehicle (HSV) can be therefore summarized as follows:

- solar energy is renewable, free and largely diffused, and Photovoltaic Panels are subject to continuous technological advances in terms of cell efficiency; their diffusion is rapidly growing, while their cost, after a continuous reduction and an inversion occurred in 2004, again shows a decreasing trend [2];
- solar cars, in spite of some spectacular outcomes in competitions as World Solar Challenge, do not represent a practical alternative to conventional cars, due to limitations on maximum power, range, dimensions and costs;
- possibility of fruitfully combining HEV- and solar power-related energetic benefits.

In next chapters, the potentialities and problems associated to Hybrid Solar Vehicle technology are presented, and some specific control issues of such vehicles discussed, based on previous work of the authors. Then, a new implementable rule-based approach for energy flow management is proposed, and the results obtained by a dynamic model are compared with those deriving by an optimal strategy obtained via Genetic Algorithms. Finally, some preliminary experimental tests are presented and discussed.

HYBRID SOLAR VEHICLES

In principle, Hybrid Solar Vehicles (HSV) could sum up the advantages of HEV and solar power, by the integration of Photovoltaic Panels in a Hybrid Electric Vehicle. But it would be simplistic to consider the development of an HSV as the simple addition of photovoltaic panels to an existing Hybrid Electric Vehicle. In fact, the development of HEV's, despite it was based on well-established technologies, showed how considerable research efforts were required for both optimizing the power-train design and defining the most suitable control and energy-management strategies. Analogously, to maximize the benefits coming from the integration of photovoltaic with HEV technology, it is required performing accurate re-design and optimization of the whole vehicle-powertrain system. In these vehicles, in fact, there are many mutual interactions between energy flows, propulsion system component sizing, vehicle dimension, performance, weight and costs, whose connections are much more critical than in conventional as well as in hybrid cars.

Another difference between HEV and HSV regards with their structure. In fact, the prevailing architectures for HEV are parallel and parallel-series, while in case of HSV the series structure seems preferable [3]. Despite some known disadvantages (higher efficiency losses due to more energy conversion stages), series structure is simpler and may offer some advantages:

- It is more suitable for plug-in and V2G applications [3] (the generator can be used as co-generator when the vehicle is parked at home).
- Due to absence of mechanical links between generator and wheels, very effective vibration insulation can be achieved, with less constraints for vehicle layout.
- Advanced techniques for noise reduction (i.e. active noise reduction) could be more easily applied, since the engine can work at fixed conditions.
- Engines specifically optimized for steady operation can be used (i.e. D.I. stratified charge engines, Micro gas turbine, and other solutions not suitable for classical vehicles due to lack of stability or low efficiency in the whole operating range).
- It is compatible with the use of in-wheel motors with built-in traction control and anti-skid.
- It will potentially act as a bridge towards the introduction of hybrid fuel cell powertrains.

A possible layout of an HSV with series structure is presented in Figure 3. The photovoltaic panels PV are usually mounted on or integrated with vehicle roof [3,4].

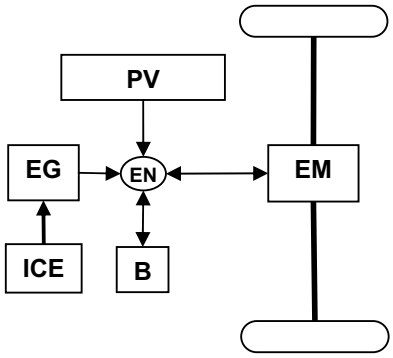

Figure 3 - *Scheme of a series hybrid solar vehicle.*

In spite of these encouraging perspectives, the use of solar energy on cars has been considered with a certain skepticism by most users, including automotive engineers. This may be due to the simple observation that the net power achievable in a car with current photovoltaic panels is about two order of magnitude less than maximum power of most of today cars. But a more careful analysis of the energy involved demonstrate that this perception may be misleading. In fact, there is a large number of drivers utilizing daily their car for short trips and with limited power demand. For instance, some recent studies conducted by the

UK government report that about 71 % of UK users reach their office by car, and 46 % of them have trips shorter than 20 minutes, mostly with only one person on board, i.e. the driver [5].

In those conditions, the solar energy collected by solar panels on the car along a day may represent a significant fraction of the energy required for traction [6-8].

Despite their potential interest, solar hybrid cars have received relatively little attention in literature [3], particularly if compared with the great effort spent in last years toward other solutions, as hydrogen cars, whose perspectives are affected by critical issues, such as production, distribution and storage.

Some prototypes have been developed in last decade in Japan [9], at Western Washington University [10], at the Queensland University [11] and, more recently, by the French company Venturi.

A prototype of Solar Prius has also been recently developed by Solar Electric Vehicles, equipped with a PV panel of 16% nominal efficiency [4]. It has been estimated that the PV Prius can have a range based on solar power alone between 5 and 8 miles per day, and that it can consume between 17% and 29% less gasoline than the standard Prius.

CONTROL ISSUES FOR HYBRID SOLAR VEHICLES

Although HSV share many common features with HEV, for which numerous studies on energy management and control have been presented in last decade [12-15], there are also some significant differences between these kind of vehicles. In particular, the presence of solar panels and the adoption of a series structure may require to study and develop specific solutions for optimal management and control of an HSV.

As it is known, in most HEV a charge sustaining strategy is adopted: at the end of a driving path, the battery state of charge should remain unchanged. With an HSV, a different strategy should be adopted as battery is charged during parking hours as well. In this case, a different goal can be pursued, namely restoring the initial state of charge within the end of the day rather than after a single driving path [8].

Moreover, the series configuration suggests to operate the engine in an intermittent way at constant operating conditions, i.e. corresponding to the minimum fuel consumption. In such case, the ICE-EG system may be designed and optimized to maximize its efficiency, emissions and noise at design point, while in current automotive engines the maximum efficiency is usually sacrificed to the need of assuring stable operation and good performance in the whole operating range. In case of ICE intermittent operation, the effects exerted on fuel consumption and emissions by the occurrence of thermal transients in engine and catalyst should be considered [8,16,17]. These effects are neglected in most studies on HEV [15] and on HSV [18], where a steady-state approach is usually preferred to evaluate fuel consumption and emissions.

In order to address the afore-mentioned control issues, in the last years the authors have performed several off-line analyses aimed at individuating optimal energy management strategies for series HSV [8,17,19,20]. Specifically in this work, the research interests and aims turned towards the development of an RB control strategy to perform quasi-optimal on-board energy management for a series HSV powertrain.

RULE-BASED CONTROL STRATEGY FOR A SERIES HYBRID SOLAR VEHICLE

The RB control architecture consists of two loops, external and internal respectively:

- external loop: defines the desired final state of charge SOC_f (see Figure 4), to be reached at the end of the driving cycle to enable full storage of solar energy capted during the following parking phase (i.e., $E_{PV,p}$).
- internal loop: estimates the average power delivered by ICE-EG and SOC deviation (dSOC) from SOC_f as function of average traction power $\overline{P}_{tr}$ and $E_{PV,p}$.

Figure 4 provides a qualitative description of the start&stop strategy enabled by the above-described control loops. For sake of simplicity, in Figure 4 it is assumed that SOC_0=SOC_f and $\overline{P}_{tr}$ does not vary with time. The battery is initially depleted until SOC becomes lower than SOC_{lo} = SOC_f-dSOC. At this point ICE-EG is turned on at the assigned power level and switches off when the maximum threshold SOC_{up} = SOC_f+dSOC is reached. The procedure is repeated until the end of the driving cycle. It is worth mentioning here that effective final state of charge may differ from the desired SOC_f due to the difficulty of precisely predicting the end of the driving phase. This consideration entails satisfying the following energetic constraint:

$$SOC_{up} + \Delta SOC_p < 1 \qquad (1)$$

where ΔSOC_p represents the state of charge increase subsequent to battery recharging performed by PV panels during parking phases.

The described control strategy relies, on one hand, on the online estimation of current SOC level and, on the other, on predicting or properly estimating $\overline{P}_{tr}$ over an assigned driving route. The following sub-sections go through a detail description of the rules defined in both external and internal loop.

EXTERNAL-LOOP RULES

As explained above, the objective of the external loop is to ensure all the available $E_{sun,p}$ be stored in the battery pack once the driving phase is over. This can be obtained imposing SOC_f always be safely lower than 1. This constraint can be expressed as follows:

$$SOC_f = 0.9 - \frac{\Delta SOC_{\max,d}}{2} - \Delta SOC_p \qquad (2)$$

where $\Delta SOC_{max,d}$ is the maximum allowed battery variation during driving phase, here assumed equal to 0.1. According to Eq. (2), at the end of the day SOC will never overcome 0.9, thus allowing to perform satisfactory battery recharging by PV panels even in the case the car is not used over an entire day (i.e. driving phase h_{car} is 0 hours long).

Of course ΔSOC_p varies with year season. Figure 5 shows the linear approximation, valid for the PV specifications listed in Table 1, of the relationship $\Delta SOC_p = f(S_f)$. S_f is a factor accounting for seasonal change of solar irradiation:

$$S_f = \frac{E_{sun,day}}{\overline{E}_{sun,day}} \qquad (3)$$

where $E_{sun,day}$ and $\overline{E}_{sun,day}$ are, respectively, the actual and year-average sunshine daily energy (see Table 1). Figure 5 also shows the variation of desired SOC_f as function of S_f, computed through Eq. (2). It is worth noting that, for S_f<0.75, SOC_f is fixed equal to 0.75.

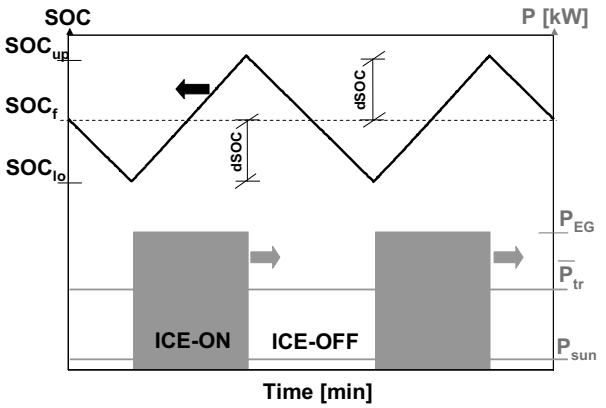

Figure 4 – *Schematic representation of the rule-based control strategy for quasi-optimal energy management of a series HSV powertrain.*

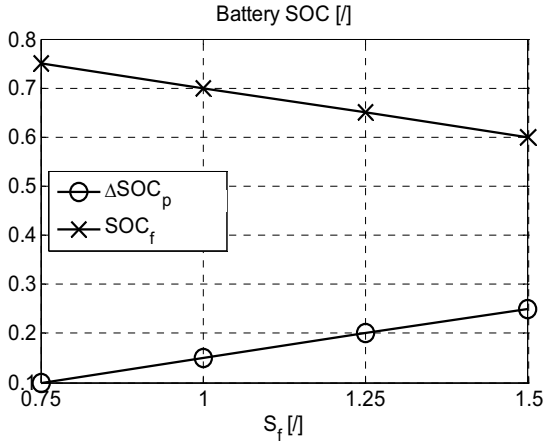

Figure 5 – *Variation of optimal final SOC as function of daily solar radiation.*

INTERNAL-LOOP RULES

Aim of this loop is to address at which power level the ICE-EG should work and how to manage its intermittent scheduling, alternating start and stop maneuvers.

The average power requested to the generator over an assigned time horizon can be determined as function of traction power, PV power and regenerative braking:

$$\overline{P}_{EG} = \overline{P}_{tr} - \overline{P}_{PV} - \overline{P}_{rb} \qquad (4)$$

The terms on the right hand side of Eq. (4) can be either estimated as function of their previous values, by means of forecast techniques such as Recursive Neural Network [12], or derived from GPS data. It is worth noting that Eq. (4) holds valid in correspondence with the electric node EN shown on Figure 3.

In case of intermittent ICE-EG scheduling, the ICE-ON and ICE-OFF duration time, respectively indicated as Δt_{ICE-ON} and $\Delta t_{ICE-OFF}$, are introduced. The time lag between two ICE-ON events can be defined as:

$$\Delta t_{crank} = \Delta t_{ICE-ON} + \Delta t_{ICE-OFF} \qquad (5)$$

The intermittent ratio can thus be introduced:

$$IR = \frac{\Delta t_{ICE-OFF}}{\Delta t_{ICE-ON} + \Delta t_{ICE-OFF}} = \frac{\Delta t_{ICE-OFF}}{\Delta t_{crank}} \qquad (6)$$

where the extreme cases IR = 0 and IR = 1 indicate, respectively, continuous ICE-ON and always ICE-OFF operation.

Then, a look-up table was developed to estimate optimal P_{EG} as function of $\overline{P}_{tr}$ and S_f. Particularly, for assigned $\overline{P}_{tr}$ and S_f, P_{EG} is determined by an optimization procedure expressed by the following equation:

$$\min_X \ \dot{m}_f\left(X, \overline{P}_{tr}, S_f\right) \qquad (7)$$

with initial condition:

$$SOC(0) = SOC_f \qquad (8)$$

and subject to the constraints:

$$SOC(\Delta t_{crank}) = SOC_f \qquad (9)$$

$$SOC > SOC_f - \Delta SOC_{\max,d} \qquad (10)$$

In Eq. (7) the decision variables X include: P_{EG}, IR and Δt_{crank}. A scalable η_{ICE} look-up table is used to map the relationship between ICE per hour fuel consumption ($\dot{m}_f$ [kg/h]) and P_{EG}. It is worth noting here that ICE fuel consumption is computed taking into account the thermal dynamics effects associated to intermittent ICE operation [8,17,19]. Moreover, the influence of $\overline{P}_{rb}$ and $\overline{P}_{PV}$ was accounted for by subtracting their value to the effective request of power at wheels.

Figure 6 shows an example of solution to the problem expressed by Eqs. (7-10). The SOC trajectory initially

decreases as the ICE-EG group is imposed to be initially off; then, due to ICE switching-on, SOC trend is inverted allowing to satisfy the constraint expressed by Eq. (9). The difference between SOC_f and SOC_{min} (see Figure 6) is used to evaluate the SOC excursion to be adopted in the rule-based control strategy depicted in Figure 4:

$$dSOC\left(\overline{P}_{tr},\, S_f\right) = \frac{SOC_f - SOC_{\min}}{2} \qquad (11)$$

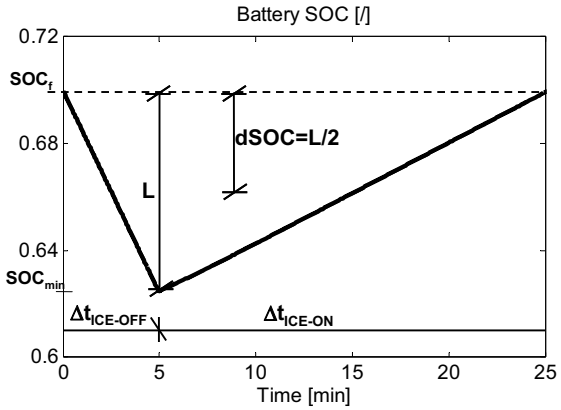

Figure 6 – *Example of solution to the optimization problem expressed by Eqs. (7-10).*

IMPLEMENTATION OF RULE-BASED STRATEGY

The overall RB control architecture consists of three look-up tables:

$$SOC_f = f\left(S_f\right) \qquad (12)$$

$$P_{EG} = f\left(\overline{P}_{tr},\, S_f\right) \qquad (13)$$

$$dSOC = f\left(\overline{P}_{tr},\, S_f\right) \qquad (14)$$

Figure 7 gives a schematic description of the rule-based control strategy implementation. Eq. (12) provides the desired SOC_f. Then, in the internal loop the average power at which the ICE-EG works is evaluated by Eq. (13). The ON-OFF rules for the ICE-EG will depend on the SOC excursion addressed by Eq. (14). The logic described in Figure 7 results in the control actions qualitatively shown on Figure 4.

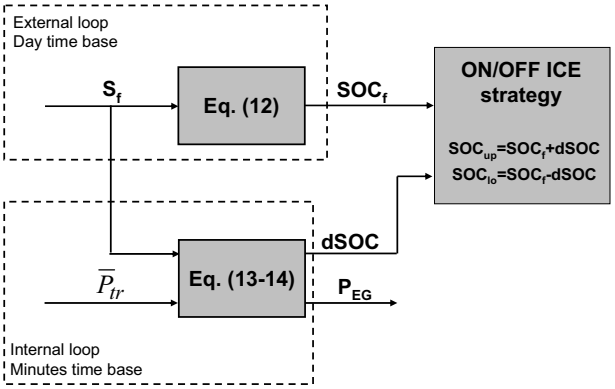

Figure 7 – *Schematic description of external and internal loop actions within the RB control strategy.*

It is worth discussing here about the determination of average traction power to be fed as input to Eqs. (13-14). One possibility is to impose $\overline{P}_{tr}$ be constantly equal to the average power demand at wheels for common driving cycles, usually in the range 5 to 10 kW for passenger cars [8]. Nevertheless, better results are expected if $\overline{P}_{tr}$ is appropriately updated during the driving route, either by inferring it from available measurements (i.e. a-posteriori knowledge) or by means of forecasting techniques (i.e. a-priori knowledge). The above cases are deeply analyzed and discussed in the results section.

SIMULATION RESULTS

The performance of the RB strategy was tested via simulation of the HSV powertrain detailed in Table 1. It was assumed that the driving phase lasts for about 4700 s (i.e. h_{car} = 1.31 h) and consists of 4 ECE-EUDC modules. The simulations were run by a longitudinal dynamical vehicle model including also engine thermal dynamics effects, previously developed by the authors [7,19,20] in Matlab® environment.

Table 1 – *HSV specifications and assumptions considered in the scenario analysis described in Table 2.*

HSV specifications	
Nominal ICE power [kW]	46
Fuel	gasoline
Nominal EG power [kW]	43
Nominal EM power [kW]	90
Number of Lead-acid battery modules	27
Battery capacity [kWh]	8
PV horizontal surface [m^2]	3
PV efficiency	0.13
Coefficient of drag (C_d)	0.33
Frontal area [m^2]	2.3
Rolling resistance coefficient [/]	0.01
Weight [kg]	1500
Scenario analysis assumptions	
$\overline{E}_{sun,day}$ at 30° Latitude [kWh/m^2]	4.31
Sun factor, S_f	1
h_{sun} [h]	10

Prior to this numerical investigation, the look-up tables expressed by Eqs. (12-14) were developed. The following intervals were selected for the independent variables: $S_f \in [0 \div 1.5]$, $\overline{P}_{tr} \in [0 \div 18]\, kW$.

Afterwards, three simulation analyses were performed referring to the three scenarios outlined in Table 2. Particularly, in scenario 1 the $\overline{P}_{tr}$ value fed to Eqs. (13-14) is never updated while in scenario 2 an a-

posteriori based knowledge is adopted to update $\overline{P}_{tr}$ as function of past $P_{tr}(t)$ measurements. On the other hand, in scenario 3 the ideal case of perfect prediction of $\overline{P}_{tr}$ in the next t_h time horizon is assumed. In scenarios 2 and 3, several simulations were performed to analyze also the effect of time-horizon length on RB performance.

In order to perform a comparative analysis of RB performance, the fuel economy yielded on output by the simulations is evaluated against a reference benchmark. Such benchmark corresponds with the genetic-algorithm-based optimization method [21] proposed by the authors in a previous contribution [20], that assumes the previous knowledge of the driving cycle. It is worth mentioning here that the GA method developed in [20] was adapted to the vehicle specifications listed in Table 1 and, more importantly, that the ICE-EG optimization degrees of freedom were increased to further reduce fuel consumption. This way, a more robust comparative assessment of RB strategy performance was guaranteed.

Figure 8 shows the variation of percent difference between simulated fuel economy and reference benchmark, evaluated as:

$$\%\Delta FE = \frac{FE_{GA} - FE_{RB}}{FE_{GA}} \cdot 100 \qquad (15)$$

As stated, Eq. (15) indicates that the more %ΔFE is, the lower are RB performances with respect to the GA benchmark. The first general result emerging from Figure 8 is that RB strategy is always competitive with the reference benchmark, with per-cent differences bounded between 0.5 and 5 % in the analyzed t_h interval. As expected, maximum performance is achieved in scenario 3, with best-case corresponding to t_h = 20 min and fuel economy only 0.5 % lower than reference benchmark. On the other hand, scenario 2 best case, which occurs at t_h = 23 min, is slightly inferior (i.e. about 3 %) to the a-priori based RB (scenarios 3 and 1, the latter also to be considered as an a-priori-based method). The comparative results reported in Figure 8 and Table 2 fully demonstrate the high potential of the proposed RB strategy, even if based on an a-posteriori knowledge of average power requested at wheels.

Figure 9 shows the time trajectories of simulated P_{tr}, P_{EG} and T_{eng} in correspondence with scenario 2 and 3 best cases (see Figure 8). As expected, in both cases it was preferable to operate the engine in the high efficiency region as much as possible (see Figure 9.a). However, the a-priori knowledge of requested power, over a significant time window of 20 minutes, allowed minimizing the number of ICE-on events in scenario 3 (4 ICE-on) as compared to scenario 2 (5 ICE-on). Moreover, scenario 3 ICE scheduling is very well managed with respect to cycle features, since ICE-on phases correspond with higher traction power demand, as shown on Figure 9.a. Regarding scenario 2, Figure 9.a clearly shows that in the beginning phase of the cycle, the lack of a-priori knowledge does not allow to select the optimal ICE operation, as it happens instead in the following phase, where scenario 2 ICE scheduling is very close to scenario 3. The latter observation can be easily explained considering that the reference cycle consists of a sequence of 4 ECE-EUDC modules. Therefore after an initial phase, a-posteriori power estimation tends to coincide to the a-priori one (see Table 2). As expected, similar comparisons can be mad regarding engine temperature and SOC trajectories, as can be noted in Figure 9.b and Figure 10. Figure 10 also indicates that during the parking phase the SOC increases over the initial value SOC_0. Such an extra battery charge ΔSOC_{ext} was accounted for in the fuel economy estimation by evaluating the equivalent fuel consumption, as follows:

$$m_{f,eq} = m_f - \frac{\Delta SOC_{ext} \cdot C_B}{\overline{\eta}_{ICE-EG} \cdot H_i} \qquad (16)$$

where $\overline{\eta}_{ICE-EG}$ is the average efficiency estimated for the ICE-EG system over the ECE-EUDC cycle.

Table 2 – *Analyzed scenarios. In the middle column i is an integer varying in the range* $\left[0 \div \frac{t_{ECE-EUDC}}{t_h}\right]$.

Scenario	$\overline{P}_{tr}$ formula	Best FE_{RB} [km/l]
1	Constant value: $\overline{P}_{tr} = \overline{P}_{ECE-EUDC}$	22.35
2	a-posteriori update: $\overline{P}_{tr}(t)\|_{t_i<t<t_i+t_h} = \frac{1}{t_h}\int_{t_i-t_h}^{t_i} P_{tr}(t)$	21.73
3	a-priori update: $\overline{P}_{tr}(t)\|_{t_i<t<t_i+t_h} = \frac{1}{t_h}\int_{t_i}^{t_i+t_h} P_{tr}(t)$	22.36

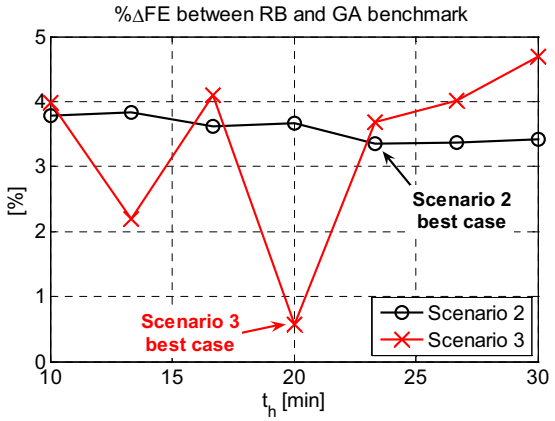

Figure 8 – *Variation of %ΔFE as function of* $\overline{P}_{tr}$ estimation *time horizon.*

Table 2 indicates that fuel economy achievable by means of the proposed RB control strategy reaches over 22 km/l. This corresponds with about 38 % fuel economy increase with respect to a conventional vehicle, the latter having same power to weight ratio as the simulated HSV (see Table 1). Moreover, the simulated HSV fuel consumptions are consistent with

other numerical results presented in previous contributions with reference to other hybrid powertrains, such as Toyota Prius, and same driving cycle (i.e. about 19 km/l on ECE-EUDC) [23]. It is also worth noting here that further fuel savings are expected upon introduction of more advanced technologies, such as lithium batteries and new generation high-efficiency PV panels and/or PV films.

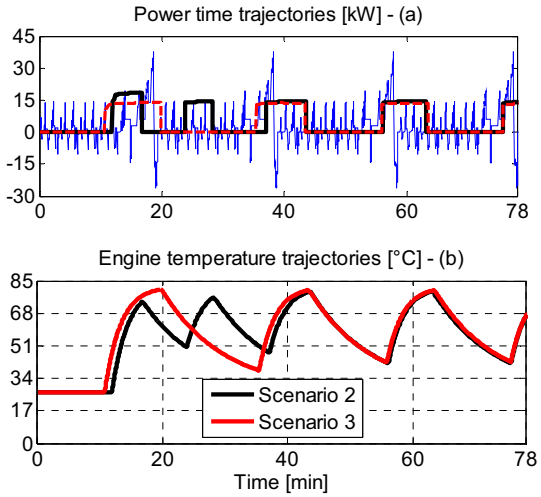

Figure 9 – *(a) Simulated power trajectories. Blu line: P_{tr}; black line: scenario 2 P_{EG}; red line: scenario 3 P_{EG}. (b) Simulated engine temperature profiles.*

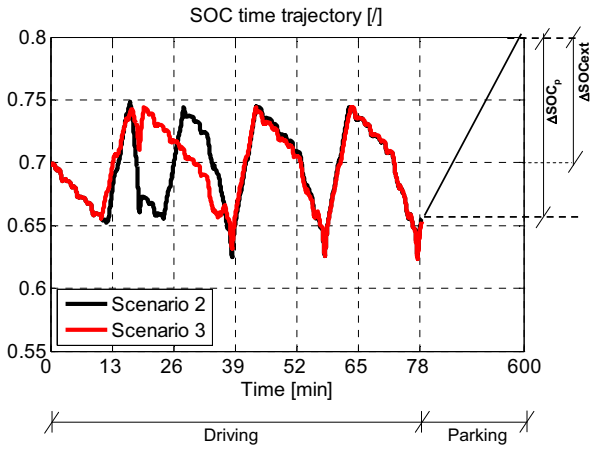

Figure 10 – *Simulated SOC profiles.*

EXPERIMENTAL TESTS

The RB control strategy is under current experimental testing on a prototype of hybrid solar vehicle previously developed by the research group [24]. Particularly, the control actions are implemented in a programmable NI-cRio® control unit, which interfaces with the real system as described in Figure 11. More in general the NI-cRrio® platform serves at the following aims:

a. Data acquisition
b. Control of ICE-EG start&stop
c. Data transfer to FTP server
d. Data transfer to SMTP server.

Regarding point b, some preliminary experimental tests were performed imposing fixed SOC_{lo} and SOC_{up} thresholds. ICE start&stop strategy can thus be introduced depending on online estimation of current state of charge. Figure 12 shows the time trajectories of main acquired signals. Particularly, Figures 12 (a) and (b) well illustrate the start&stop strategy enabled by the NI-cRio® controller by acting on the corresponding switching relays. It is worth remarking here that PV power trajectory (whose values were very low when the experiment was carried-out) was omitted in Figure 12 for sake of clarity.

An interesting feature of the available HSV test bench is represented by the torque meter (see Figure 12.e), which allows precise estimation of traction power demand, on one hand, and to deeply assess regenerative braking contribution, on the other.

The experimental test described in Figure 12 resulted in a fuel economy up to 14 km/l.

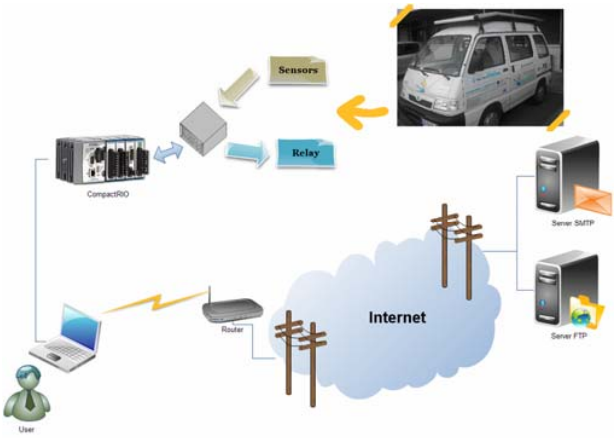

Figure 11 – *Schematic description of the data acquisition/controller developed in NI-cRio environment for the HSV prototype [24].*

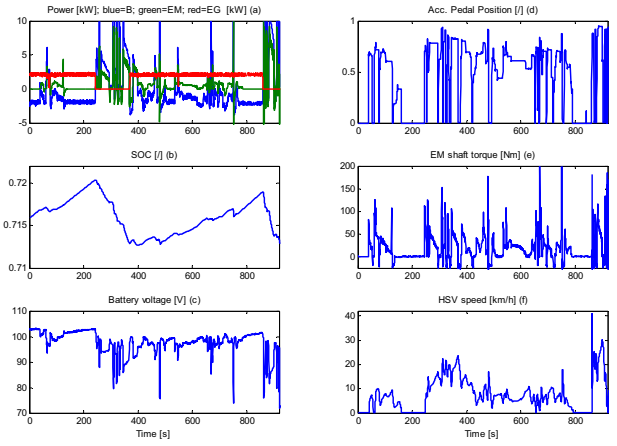

Figure 12 – *Preliminary experimental testing of RB strategy for HSV energy management.*

CONCLUSIONS

The paper presents a rule-based methodology for quasi-optimal on-board energy management of series hybrid solar vehicles. Suited numerical procedures were set-up to develop heuristic rules aimed at varying

the start&stop strategies of the ICE-EG system as function of expected traction power demand and solar radiation.

The developed control architecture consists of two main loops. The outer level (i.e. external loop) estimates, on a daily time base, the final state of charge to be reached at the end of the driving cycle. This way, it is ensured that the battery will fully recovery the solar energy captured during the following parking phase. At the inner level (i.e. the internal loop) real time estimation of quasi-optimal EG power and SOC deviation as function of current power demand and expected solar irradiation is performed.

Extensive simulations were carried out to test the proposed RB strategy. The potentialities offered by such an approach were successfully demonstrated via comparison with fuel savings evaluated by means of genetic-algorithm-based optimization of ICE scheduling on the same driving cycle (i.e. ECE-EUDC). The numerical analyses also indicated that RB achieves satisfactory performance even without predicting future power demands. Of course, the availability of forecasting models will guarantee further improvement of RB performances.

Future work will focus, on one hand, on extending the numerical analyses to other driving cycles and/or HSV architecture and, on the other hand, on further testing real world performance of the proposed RB strategy on an HSV prototype.

REFERENCES

[1] The Kyoto Protocol, http://unfccc.int/kyoto_protocol/items/2830.php
[2] Retail PV costs, www.solarbuzz.com
[3] Letendre S., Perez R., Herig C. (2003), Vehicle Integrated PV: A Clean and Secure Fuel for Hybrid Electric Vehicles, Proc. of the American Solar Energy Society Solar 2003 Conference, June 21-23, 2003, Austin,TX.
[4] Simburger J.T., Simburger E.J., Greg Johanson G., Bagnall M. (2006), “PV Prius”, Conference Record of the 2006 IEEE 4th World Conference on Photovoltaic Energy Conversion, WCPEC-4 2, art. no. 4060162, pp. 2404-2406.
[5] Statistics for Road Transport, UK Government, www.statistics.gov.uk/CCI/nscl.asp?ID=8100.
[6] Arsie I., Marotta M., Pianese C., Rizzo G., Sorrentino M. (2005); Optimal Design of a Hybrid Electric Car with Solar Cells, Proc. of 1st AUTOCOM Workshop on Preventive and Active Safety Systems for Road Vehicles, Istanbul, Sept.19-21, 2005.
[7] Arsie I., Rizzo G., Sorrentino M. (2006), Optimal Design of a Hybrid Solar Vehicle, AVEC06 - 8th Intl. Symp. on Advanced Vehicle Control - August 20-24, 2006 - Taiwan
[8] Arsie I., Rizzo G., Sorrentino M. (2007) Optimal Design and Dynamic Simulation of a Hybrid Solar Vehicle, SAE TRANSACTIONS - JOURNAL OF ENGINES 115-3: 805-811
[9] Saitoh, T.; Hisada, T.; Gomi, C.; Maeda, C. (1992), Improvement of urban air pollution via solar-assisted super energy efficient vehicle. 92 ASME JSES KSES Int Sol Energy Conf. Publ by ASME, New York, NY, USA.p 571-577.
[10] Seal M.R., Campbell G. (1995), Ground-up hybrid vehicle program at the vehicle research institute. Electric and Hybrid Vehicles - Implementation of Technology SAE Special Publications n 1105 1995.SAE, Warrendale, PA, USA.p 59-65.
[11] Simpson A., Walker G., Greaves M., Finn D. and Guymer B., (2002) “The UltraCommuter: A Viable and Desirable Solar-Powered Commuter Vehicle”, Australasian Universities Power Engineering Conference, AUPEC’02, Melbourne, Sep 29 – Oct 2, 2002.
[12] Arsie, I., Graziosi, M., Pianese, C., Rizzo, G., Sorrentino, M., (2005), “Control Strategy Optimization for Hybrid Electric Vehicles via Provisional Load Estimate”, Review of Automotive Engineering, ISSN 1349-4724, Vol. 26, pp. 341-348.
[13] Baumann B., Rizzoni G. and Washington G. (1998), Intelligent Control of Hybrid Vehicles using Neural Networks and Fuzzy Logic. SAE paper 981061, 1998.
[14] Powell B.K., Bailey K.E., Cikanek S.R. (1998), Dynamic modeling and Control of Hybrid Vehicle Powertrain Systems. IEEE Transactions on Control Systems, vol. 18, no. 5, 1998.
[15] Guzzella L. and Amstutz A. (1999), CAE Tools for Quasi-Static Modeling and Optimization of Hybrid Poweretrains. IEEE Transactions on Vehicular Technology, vol. 48, no. 6, November 1999.
[16] Ohn H., Yu S., Min K.D.(2008), “Effects of Spark Ignition Timing and Fuel Injection Strategy for Combustion Stability on HEV Powertrain During Engine Restart and Deceleration Driving”, Proc .of IFAC World Congress 2008, July 6-11, 2008, Seoul, pp. 5658-5663.
[17] Arsie I., Di Martino R., Rizzo G., Sorrentino M. (2007) “Toward a Supervisory Control of a Hybrid Solar Vehicle” In: IFAC Symposium "Advances in Automotive Control" AAC07, August 20-22, 2007, Monterey (CA) Edited by:Elsevier.
[18] Preitl Z., Bauer P., Kulcsar B., Rizzo G., Bokor J. (2007) Control Solutions for Hybrid Solar Vehicle Fuel Consumption Minimization In: Proceedings of the 2007 IEEE Intelligent Vehicles Symposium, Istanbul, Turkey, June 13-15, 2007.
[19] Arsie I., Di Martino R., Rizzo G., Sorrentino M (2008), “Energy Management for a Hybrid Solar Vehicle with Series Structure”, Proc. of 17th IFAC World Congress, July 6-11, 2008, Seoul.
[20] Arsie I., Di Martino R., Rizzo G., Sorrentino M. (2008), On the use of genetic algorithm to optimize the on-board energy management of a hybrid solar vehicle, "Les Rencontres Scientifiques de l'IFP - Advances in Hybrid Powertrains", 25-26 November 2008, IFP/Rueil-Malmaison, France.
[21] Chipperfield, A.J., Fleming, P.J., Polheim, H., Fonseca, C.M., “Genetic Algorithm Toolbox – Matlab Tutorial”, Department of Automatic Control and System Engineering - University of Sheffield, www.shef.ac.uk/acse/research/ecrg/getgat.html.
[22] Burch, S., Cuddy, M., Johnson, V., Markel, T., Rausen, D., Sprik, S., and Wipke, K., (1999),

"ADVISOR: Advanced Vehicle Simulator", available at: www.ctts.nrel.gov
[23] Molyneaux A., Leyland G., Favrat D. (2003), Multi-Objective Optimisation of Vehicle Drivetrains, 3rd Swiss Transport Research Conference, Monte Verita / Ascona, March 19-21, 2003.
[24] www.eprolab.unisa.it.

CONTACT

Gianfranco Rizzo (grizzo@unisa.it)

Marco Sorrentino (msorrentino@unisa.it)

Ivan Arsie (iarsie@unisa.it)

Tel. +39 089 964080 – Fax +39 089 964080

Web www.eprolab.unisa.it

DEFINITIONS, ACRONYMS, ABBREVIATIONS

B: Battery

C_B: Battery capacity (J)

EG: Electric generator

EM: Electric motor

EN: Electric node

FE: Fuel economy (km/l)

GA: Genetic algorithm

h_{car}: Driving hours (h)

h_{sun}: Solar energy daily availability (h)

H_i: Gasoline lower heating value (J/kg)

HSV: Hybrid solar vehicle

ICE: Internal combustion engine

m_f: Fuel consumption (kg)

P: Power (W)

P_{EG}: EG Power (W)

P_{tr}: Traction Power (W)

PV: Photovoltaic

RB: Rule base

SOC: Battery state of charge

SOC_f: Desired SOC at driving phase end

t_h: $\overline{P}_{tr}$ estimation time horizon (min)

T_{eng}: Engine temperature (°C)

η_{ICE}: ICE efficiency

%ΔFE: percent fuel economy difference

$\bar{x}$: average value of the generic variable x